

The Malaysian International Tribology Conference 2013, MITC2013

## Three Dimensional Computational Study for spiral Dry Gas Seal with Constant Groove Depth and Different Tapered Grooves

Ibrahim Shahin<sup>a,\*</sup>, Mohamed Gadala<sup>b</sup>, Mohamed Alqaradawi<sup>c</sup>, Osama Badr<sup>d</sup>

<sup>a</sup>Mechanical and industrial Engineering department, Collage of Engineering, Qatar University, Doha (2713), Qatar

<sup>b</sup>Mechanical Engineering department, UBC-University of British Columbia, Vancouver, BC, Canada

<sup>c</sup>Mechanical Engineering department, UBE-University of British Egypt

### Abstract

The three dimensional simulation for dry gas seal with constant depth spiral grooves and with different taper grooves is done using ANSYS FLUENT CFD code. Grid independence study and code validation are done with experimental work. The fluid state effect on the gas seal internal flow and performance is studied. The laminar and turbulent flow with RNG K- $\epsilon$  turbulence model and LES is examined for the same geometrical and operating conditions. The influence of film thickness for constant depth groove gas seal is simulated for 2, 3 and 4  $\mu\text{m}$  film. The effect of different rotational speeds on gas seal performance is examined for 0, 2500, 5000, 7500 and 10380 rpm. Three taper spiral grooves are studied each with three different angles, including taper grooves in the radial, circumferential and combined radial-circumferential directions. The laminar flow simulation for the dry gas seal agree well with the experimental results more than the turbulent flow simulation which overestimate the pressure distribution inside the seal. The results indicate that as the rotational speed increases the seal open force and leakage increase. The use of tapered type spiral groove causes a reduction in the seal open force and the leakage rate. Increasing the angle of radial taper groove reduces the temperature distribution inside the gas film. The reduction in seal open force and leakage rate is higher when the combined radial-circumferential taper is more than radial and circumferential taper used.

© 2013 The Authors. Published by Elsevier Ltd. Open access under [CC BY-NC-ND license](https://creativecommons.org/licenses/by-nc-nd/4.0/).

Selection and peer-review under responsibility of The Malaysian Tribology Society (MYTRIBOS), Department of Mechanical Engineering, Universiti Malaya, 50603 Kuala Lumpur, Malaysia

*Keywords:* Computational study, dry gas seal, performance, tapered spiral groove

### Nomenclature

B	land region width
$b_1$	Groove width
h	groove depth $\mu\text{m}$
$P_i$	inner pressure
$P_o$	outer pressure
$R_g$	Groove radius mm
$R_i$	Seal face inner radius mm
$R_o$	Seal face outer radius mm

T	Temperature
U	Rotating face tip speed m/s
V	Velocity m/s
<i>Greek symbols</i>	
$\Theta$	circumferential coordinate attached to rotating face
$\delta$	Gas film thickness $\mu\text{m}$
$\omega$	the angle velocity of the rotator rpm
$\beta$	land to groove area ratio $\beta=b_1/b$
$\gamma$	clearance ratio
$\alpha$	spiral groove angle
$\varphi$	taper angle

## 1. Introduction.

Leakage is a wide spread phenomenon in the oil and gas production rotating machines. It not only can cause a waste of supplies and energy, but also threats to the safety of people around, due to flammable, explosive, corrosive, toxic working fluid. Advanced sealing technology is the only way to solve the problem. Dry gas seal is a kind of non-contacting dynamic seal used for sealing of rotating shafts. It gets wide applications in petroleum and chemical industries, especially in centrifugal compressors because of high stability and low maintenance. The location of DGS in a typical centrifugal compressor is shown in Fig. 1(a); it is located at the interface between the inside of the compressor and the atmosphere. The seals are fed with a clean, heated if necessary and dry gas usually taken at the discharge of the compressor. [1]

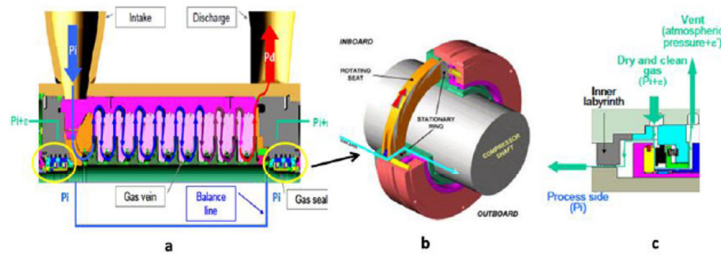


Fig.1. Dry gas seal (a) Centrifugal compressor cross section, (b) cut way for dry gas seal, (c) cross section of simplified dry gas seal. [1]

A simplified gas seal cut away and cross section is shown in Fig. 1(b) and Fig. 1(c), the leakage is forced to pass between a static and a rotating part. When the shaft rotating, an aerodynamic pumping effect generated by the grooves and creates a very small gap between the rotating and stationary faces. Bing, et al. [2], made a CFD study for turbulence effects and methods for their evaluation which are not considered in the existing industrial designs of dry gas seal. Jing, et al. [3], make a CFD study for the three dimension micro-scale flow field in spiral groove dry gas seals (S-DGS). Effect of gas flow state on the Seal performance is analysed under different gas film thickness. Bing and Huiqiang [4] investigate the micro scale effects on spiral groove dry gas seal performance in a numerical solution of a corrected Reynolds equation. Miller, B., and Green, I., [6] developed two new methods for characterizing the properties of gas lubricated mechanical face seals. Results from both methods agree well with previously published results computed using the perturbation method. Glienicke et al., [7] developed mathematical fundamentals concerning the Calculation of non-contacting gas lubricated face seals. The tests were performed with three seal designs at operating pressures pop up to 10 MPa and sliding velocities  $v$  up to 110 m/s. Numerical simulation is carried out by Heshun, W. and Cichang, C. [8], based on the Navier-Stokes (N-S) equation, the laminar model. Five geometric parameters are investigated and use one by one optimize method, take opening force, leakage, gas film stiffness and the ratio of stiffness and leakage as the assessing target. Heshun, et. al. [9], made a numerical simulation of face flow filed under different face clearances, based on the Navier Stokes equation, the laminar model. Hydrodynamic pressure weakens rapidly as face clearance increased and changes acutely at small clearance (less than  $3\mu\text{m}$ ) zone. From the review of some of works done on dry gas seal, common shortage in these

studies such as, the computational model simplified too much. Mostly consider the flow field as a 2-D model. Also for 3D studies the grid is scaled with a factor in the axial direction. Also most of the studies are done for the standard design for the spiral groove dry gas seal with little care with the analysis of the film internal flow field especially pressure, velocity and temperature distribution, and Also spiral dry gas seal need more modifications to be suitable for wide operating conditions.

## 2. Governing equations and turbulence model.

Three-dimensional, steady Reynolds-averaged Navier-Stokes equations are solved. For a 3-dimensional, steady, incompressible for the velocity field  $V = (V_1, V_2, V_3)$  expressed in a reference Cartesian co-ordinate system  $x = (x_1, x_2, x_3)$ : the continuity equation (1), conservation of momentum (2) and energy equation, can be written as follows:

$$\frac{\partial(\rho \bar{V}_i)}{\partial x_i} = 0 \quad (1)$$

$$\frac{\partial(\rho \bar{V}_i)}{\partial t} + \frac{\partial(\rho \bar{V}_i \bar{V}_j)}{\partial x_j} = -\frac{\partial \bar{P}}{\partial x_i} + \mu \frac{\partial}{\partial x_j} \left( \frac{\partial \bar{V}_i}{\partial x_j} + \frac{\partial \bar{V}_j}{\partial x_i} \right) - \frac{\partial(\rho \bar{V}_i' \bar{V}_j')}{\partial x_j} \quad (2)$$

Where:  $p$  is the static pressure,  $V_i$  denotes a velocity component and  $x_i$  stands for a coordinate direction. The turbulence is simulated by the K- $\epsilon$  RNG turbulence model with non-equilibrium near wall treatments, with 2% turbulence intensity at flow inlet. The FV discretization in space is of second order accuracy. The solution residuals is set less than  $10e-4$ , the seal performance parameters are monitored while iteration to confirm solution convergence.

## 3. Model description and boundary conditions.

The model is used to simulate the fluid between the rotating and stationary faces of the dry gas seal. Fig.2a shows the basic geometrical parameters of the simulated domain. The computational domain and grid generation are done by GAMBIT pre-processor shown in Fig. 2(b) and Fig. 2(c) in which the fluid domain is magnified by 1000 times in the groove depth direction only to show geometry and grid detail. While calculations the dimensions are not scaled. The pressure inlet boundary condition is used at the inlet for the fluid, the pressure outlet boundary conditions is used at the domain outlet, the rotating periodic boundary condition is used and the wall boundary condition is used for both the rotating and stationary gas seal faces. The no slip velocity conditions are employed at the walls as the Kundsens number is less than 0.001 [2]. The single rotating reference frame model is used to model the fluid rotation. The code is validated with experimental and numerical work of [11] with the same geometric and operating conditions, Also these geometrical parameters are used for the present study. The hexahedral elements are used for domain meshing, using cooper method.

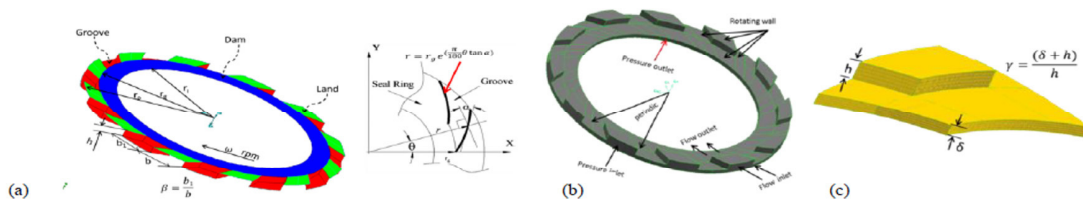


Fig. 2. Basic geometric parameters for dry gas seal (a) spiral groove, (b) Basic computational domain boundary conditions and (c) domain mesh.

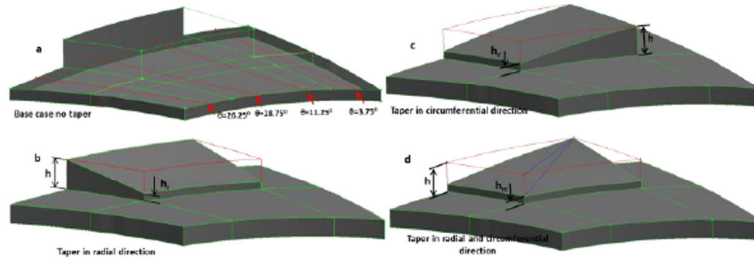


Fig. 3. Domain for case without taper and cases with taper groove.

## 4. Results and discussion

### 4.1 Code validation and grid independence study

In order to ensure the accuracy of numerical solution, a careful check for grid independence should be conducted. Three numbers of computational nodes are used 1.17, 1.8 and 2.173 million of nodes. The pressure along the radial direction is plotted in Fig.4a for present simulation with different number of nodes and the experimental results of [11]. The present results with 1.17 million nodes agree well with experimental data from [11], and no change in results noted by increasing the nodes to 1.8 million, whereas the solution with more number of nodes 2.173 million is less accurate and cause a slightly over estimation of the pressure near the groove root. So the grid with 1.17 million nodes is used for all the studies conducted in the later sections. The influence of fluid state is done by simulating the flow as a laminar flow and as turbulent flow with using different turbulence model. The pressure along the radial direction is plotted in Fig. 4(b) for laminar and turbulent flow calculations. The Laminar flow results agree well with experimental data from literature [11], whereas the solutions of the turbulent flow using K- $\epsilon$  turbulence model or large eddy simulation are less accurate. The turbulent calculation overestimates the peak value of the gas film pressure. So the laminar flow calculations are used for all the studies conducted in the later sections.

### 4.2 Influence of gas film thickness

In this study, the seal geometrical and operation parameters is kept constant and the film thickness is varied from 2  $\mu\text{m}$ , 3  $\mu\text{m}$  and 5  $\mu\text{m}$ . the normalized static pressure distribution for different film thickness is shown for Fig. 5(a). The gas film thickness has great effect on pressure and this effect is getting greater as the gas film thickness is reducing as the effect of dynamic pressure is increasing. The pressure peak forms in the boundary of spiral groove and seal dam is increased by reduction in film thickness. Conversely, when gas film thickness is deeper, the gas film pressure will decrease, and the pumping effect of spiral groove is slighter even disappear. The decrease of film thickness causes an increase in the temperature distribution inside the gas film as shown Fig.5b, the increase in the temperature is more clear when the film thickness decreases from 3  $\mu\text{m}$  into 2  $\mu\text{m}$ . The effect of changing film thickness on the gas seal performance parameters is shown in Fig. 6(a) and Fig. 6(b), the seal open force decreases as the thickness of the film becomes greater, this is as a result of film stiffness which decrease as the film thickness increase. The leakage rate increases with the increase in the film thickness.

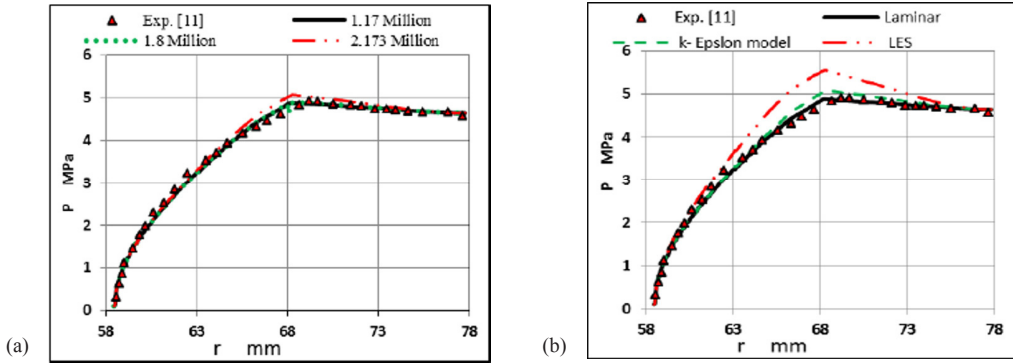


Fig. 4. Static pressure distribution in radial direction for (a) different no. of computational nodes and (b) laminar flow and different turbulence model.

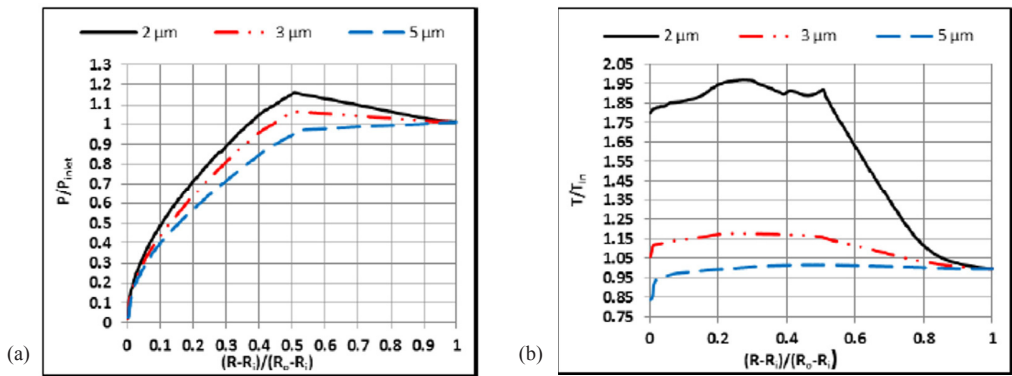


Fig. 5. Gas film thickness effect on (a) Normalized static pressure distribution at  $\Theta=11.25^\circ$ , (b) Normalized temperature distribution at  $\Theta=11.25^\circ$

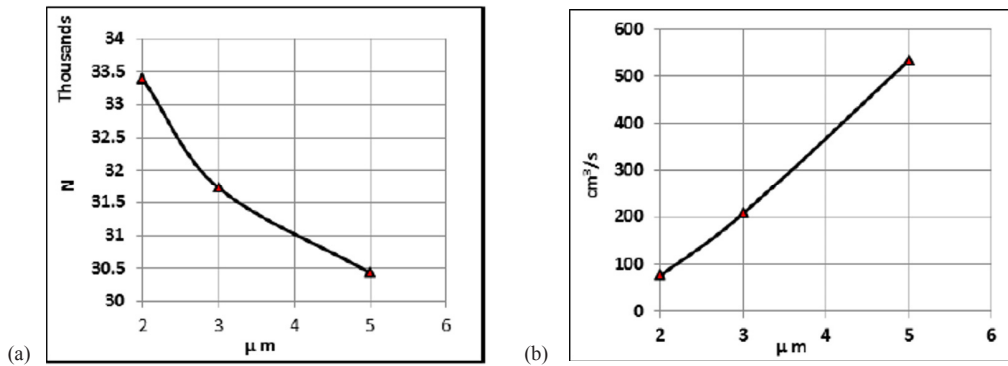


Fig.6 Gas film thickness effect on (a) open force and (b) Gas seal leakage volume flow rate

### 4.3 Influence of using Radial taper groove

To examine the effect of using radial taper groove on the gas seal performance, the simulation is done for the gas seal with the same geometrical parameters except that the groove depth is decreased in the radial direction by ratio  $h_r/h$ , the rotating face geometry and the computational domain are shown in Fig. 3. Four cases are studied with ratio 1, 0.75, 0.5 and 0.25; by decreasing this ratio the groove height at the gross is decreased. The radial taper groove has a small effect on the pressure distribution in radial direction Fig. 7(a), as the taper angle increase the pressure distribution decreases and the pressure peak decreases. Fig. 7(b) shows the effect of radial taper groove angle on the temperature distribution, and it is clear that the temperature decreases with increasing the taper angle especially at the groove end and seal dam area. This is thought to be due to the fluid exchange between the groove and the fluid film on top of the grooves. As the groove tapered with high angle, the area of the groove contact with the gas system is larger, and the fluid exchange between the groove and the fluid film becomes greater. Consequently heat is then carried through convective heat transfer, thus resulting in a lower fluid temperature and seal temperature. Fig. 8(a) illustrates how the seal open force varies with groove taper angle and speed. At low groove taper angle, the open force is high and as the groove taper angle becomes greater, the open force decreases rapidly. The leakage rate also decreases with increasing the taper groove angle Fig. 8(b). This means that if one desires a low leakage rate and a low seal temperature, then high angle taper groove is required. If low friction and wear is preferred, then groove without taper or small taper grooves should be applied.

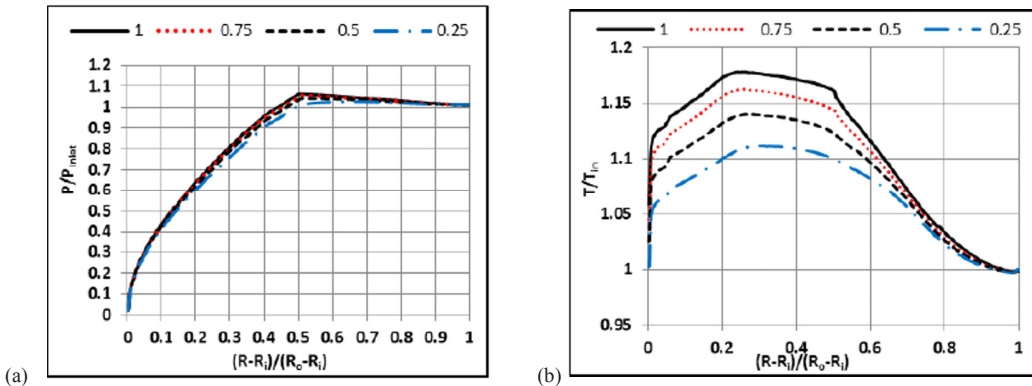


Fig. 7. Radial taper with different depth reduction ratio effect on (a) Normalized static pressure (b) Normalized temperature.

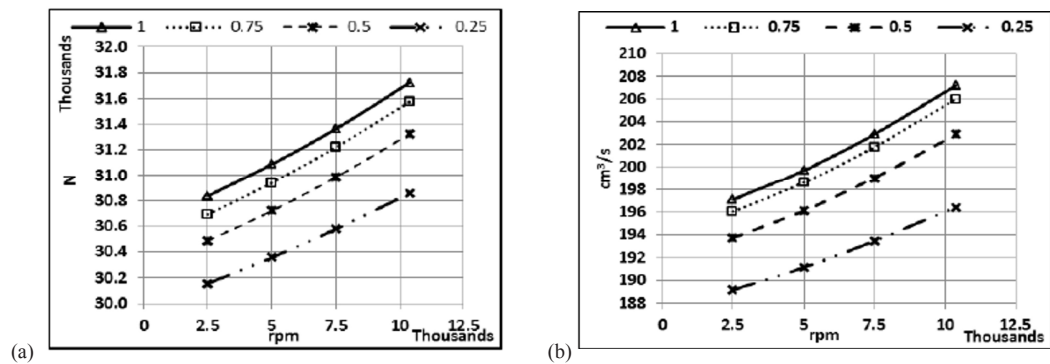


Fig. 8 Radial taper with different depth reduction ratio effect on (a) Open force (b) Leakage rate.

4.4 Influence of using circumferential taper groove

In this numerical simulation the groove depth is decreased gradually in the circumferential direction with ratio  $h_c/h = 1, 0.75, 0.5$  and  $0.25$  with the rotation direction as shown in Fig.3. Figure 9 show that the circumferential taper groove has a negative effect on the open force of a seal. With increasing taper angle, the open force decreases. Also the leakage rate decreases with using circumferential taper, especially at high taper angle, as a result of flow area across the groove.

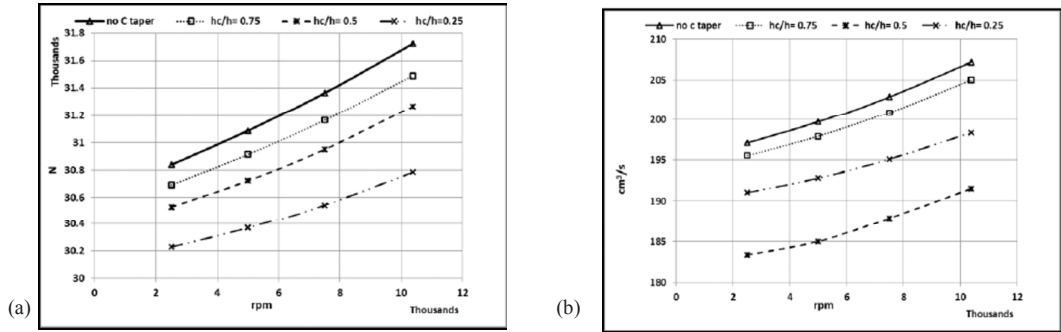


Fig. 9. Circumferential taper with different depth reduction ratio effect on (a) Open force (b) Leakage rate.

4.5 Influence of using combined radial and circumferential taper groove

To examine the effect of combined radial and circumferential taper groove on the seal performance, simulation is done for grooves with three taper angles with ratio  $h_{rc}/h = 1, 0.75, 0.5$  and  $0.25$  shown in Fig. 3 in both radial and circumferential direction. Fig. 10(a) shows the effect of combined taper on the seal open force, as the combined taper angle increases the open force decrease. This decrease is slightly affected by the rotational speed, it can be seen that at high speed the decrease in open force is higher than that at lower speed. The leakage rate for different combined taper groove angles is illustrated in Fig. 10(b), as the taper angle increased the seal leakage decreased. As taper angle increases the friction area from groove inlet to groove end increased, that result in generating higher pressure drop across the grooves causing lower leakage rate. The performance results are drawn for the same taper angle but for different taper type. Fig. 11 shows that the decrease in open force when combined taper is used is more than each of radial or circumferential taper used. The open force remains the same for radial and circumferential taper. At the same time the decrease in leakage rate for circumferential taper is much more the decrease when using radial taper grooves.

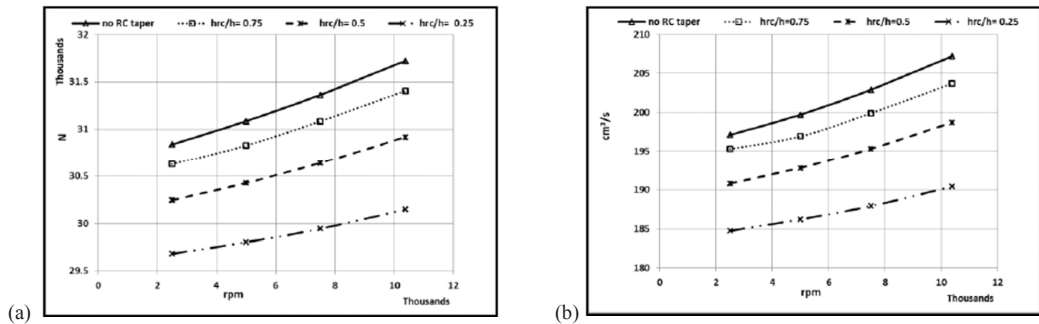


Fig.10. Combined radial and circumferential taper with different depth reduction ratio effect on (a) Open force (b) Leakage rate.



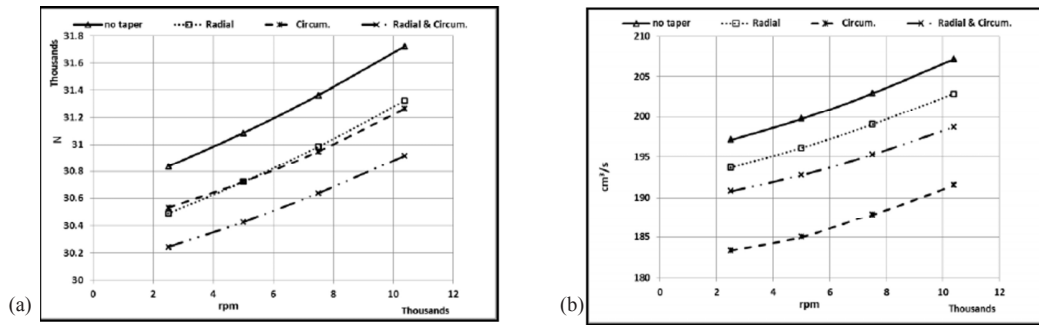


Fig.11. Taper type with 0.5 reduction ratio effect on (a) Open force (b) Leakage rate.

#### 4. Conclusion

A three dimensional CFD model is developed to study the effect of operating parameters such as the fluid state, the film thickness and the rotational speed on the gas seal performance and internal flow field. Geometrical parameters including the constant depth seal groove, radial taper groove angle, circumferential groove angle and combined radial-circumferential taper angle are studied. The laminar flow results agree well with the experimental data whereas the solutions of the turbulent flow using K- $\epsilon$  turbulence model or large eddy simulation are less accurate. The pressure peak forms in the boundary of spiral groove and seal dam is increased by reduction in film thickness. Conversely, when gas film thickness is deeper, the gas film pressure will decrease, and the pumping effect of spiral groove can even disappear. The decrease of film thickness causes an increase in the temperature distribution inside the gas film. The radial taper groove has a small effect on the pressure distribution and increases the taper angle thus causes a noticed decrease in the temperature distribution inside the seal.

#### Acknowledgement

This publication was made possible by NPRP grant No. 4-651-2-242 from the Qatar National Research Fund (a member of Qatar Foundation). The statements made herein are solely the responsibility of the authors.

#### References:-

- [1] Gad, A., 2011. Reverse Rotation in Centrifugal Compressors. Proceedings of the 40<sup>th</sup> Turbo-machinery Symposium, 12-15 September – Houston, TX
- [2] Bing, W., Huiqiang, Z., and Hongjun, C., 2012. Flow Dynamics of a Spiral groove Dry gas Seal. Chinese Mechanical Engineering Society and Springer Verlag Berlin Heidelberg 2012, DOI: 10.3901/CJME.
- [3] Jing, X., Xudong, P., Shaoxian, B., Xiangkai, M., 2012. CFD Simulation of Micro scale Flow Field in Spiral Groove Dry Gas Seal. 978-1-4673-2349-9/12, IEEE.
- [4] Bing, W., and Huiqiang, Z., 2011. Numerical Analysis of a Spiral groove Dry gas Seal Considering Micro scale Effects” Chinese Journal of Mechanical Engineering, DOI: 10.3901/CJME.2011.
- [5] Hifumi, T., and Mitsuo, S., 2005. Development of High-Speed and High-Pressure Dry-Gas-Seal. IHI Engineering Review, Vol. 38 No. 1 2005.
- [6] Miller, B., and Green, I., 2002. Numerical Techniques for Computing Rotor dynamic Properties of Mechanical Gas Face Seals. Journal of Tribology, ASME, Vol. 124 - 755, DOI: 10.1115/1.1467635.
- [7] Glienicke, J., Lauert, A., Schlums, H., and Kohring, B., 1994. None contacting gas lubricated face seals for hug P-V values. N95-13609.
- [8] Heshun, W. and Cichang, C., 2009. Numerical Simulation on the Geometric Parameters of Spiral Grooved Dry Gas Seals. Proceedings of International Colloquium on Computing, Communication, Control, and Management, 978-1-4244-4246-1/09, IEEE.
- [9] Heshun, W., Weibing, Z, Qiang, W., Zepei, H., and Chening, Z., 2010. Numerical Simulation on Flow Field of Spiral Grooved Dry Gas Seals. Proceedings of International Conference on Computer Design and Applications (ICDDA 2010). 978-1-4244-7164-5.
- [10] Weibing, Z., Heshun, W., Shengren, Z. and Xiuqin, C., 2009. Research on Face Fluid Field and Seal Performance of T-shape Groove Dry Gas Seal. Proceedings of Second International Conference on Intelligent Computation Technology and Automation, 978-0-7695-3804-4/09.
- [11] Gabriel, R., 1994. Fundamentals of spiral groove non-contacting face seals. Journal of Lubrication Engineering, 50(3): 215-224.